

PFC/JA-86-46

**Čerenkov-Electrooptic Shutter—A Subnanosecond  
Intense, Relativistic Electron Beam Diagnostic**

F. Hartemann and G. Bekefi

July 1986

Plasma Fusion Center  
Massachusetts Institute of Technology  
Cambridge, Massachusetts 02139 USA

This work was supported by the Lawrence Livermore National Laboratory, the Air Force Office of Scientific Research, the National Science Foundation and the Department of Energy.

Submitted for publication to Applied Physics Letters.

**Čerenkov-Electrooptic shutter — A subnanosecond  
intense, relativistic electron beam diagnostic**

*F. Hartemann† and G. Bekefi*

Department of Physics and Research Laboratory of Electronics,  
Massachusetts Institute of Technology  
Cambridge, Massachusetts, 02139

**Abstract**

A Čerenkov-electrooptical diagnostic of intense, relativistic electron beams, giving two-dimensional images with subnanosecond resolution is described. The technique is applied to the measurements of the electron beam emittance from a multielectrode field emission gun (2 MV, 1 kA, 30 ns), and to the study of the stability of a rotating relativistic electron ring (200 kV, 100 A, 1  $\mu$ s).

---

† Permanent address : *Laboratoire de Physique des gaz et des Plasmas, Université Paris-Sud, Centre d'Orsay, France*

Two-dimensional spatial display with subnanosecond time resolution described in this letter is of interest in several areas of intense, relativistic electron beam research. For example, intense relativistic electron beams are prone to various instabilities<sup>1</sup> with growth times of tens to hundreds of picoseconds. Even if the electron beam is macroscopically stable, the beam quality, namely the emittance and brightness<sup>2</sup> may well be strongly time-dependent. Such is the case of electron beams produced by guns with field emission cathodes<sup>3</sup>, photoelectric cathodes<sup>4</sup> and laser driven field emission cathodes<sup>5</sup>.

In this letter we describe a new diagnostic, with subnanosecond temporal resolution, and giving high quality two-dimensional images on regular 35 mm film. The principle of operation is the following : sampling of the "fast" Čerenkov radiation emitted by the electrons incident on a Plexiglass sheet, followed by an electrooptic crystal gated for a few hundred picoseconds. For very fast events, the number of photons propagating in the device is very small and a microchannel array image intensifier (MCP) is used to enhance the sensitivity ; it also helps to increase the contrast of the system (double gating process : high contrast, slow gate of the MCP superimposed on the fast gate of the electrooptic crystal).

As a proof of principle, this diagnostic has been applied to the time-resolved measurement of the beam emittance from a multielectrode field emission gun (2 MV, 1 kA, 30 ns)<sup>6,7</sup>, and to the study of the stability of a rotating, relativistic electron ring<sup>8</sup> (200 kV, 100 A, 1  $\mu$ s).

The experimental setup is illustrated in Fig. 1. The electron beam under study is incident normally on a Plexiglass sheet (10 cm  $\times$  10 cm, 3-10 mm thick) coated on the beam side with graphite (Aerodag) so as to prevent direct light from the cathode-anode gap from reaching the optical system. The Čerenkov light emitted by the electrons in the Plexiglass is viewed through a plane mirror set at 45° to the electron beam axis. This minimizes X-ray flux from entering the optical device. Further reduction of the X-ray background is achieved by lead shielding of all sensitive components.

The light leaving the mirror is collimated by lenses  $L_1$  (focal length  $f_1 = 5$  cm) and  $L_2$  ( $f_2 = 20$  cm) and impinges on the electrooptical shutter (Lasermetrics Model 1041 FW E-O Modulator) comprised of a polarizer, analyzer and a  $KD^*P$  crystal energized in the longitudinal configuration<sup>9</sup>. Subsequently, the light is focussed by means of lens

$L_3$  ( $f_3 = 30$  cm) onto the microchannel array of the MCP (Varo Electron Devices # 5772 Image Intensifier) comprised of a 400 channels/mm<sup>2</sup> array distributed on a 3 cm<sup>2</sup> area, and having a gain of  $\sim 10^4$ . The amplified image produced on a scintillator screen is photographed on regular 35 mm film.

The  $KD^*P$  crystal is triggered with a  $\Delta\tau_1 = 750$  ps, 2–6 kV voltage pulse and the MCP is triggered with a  $\Delta\tau_2 = 12$  ns, 800 V pulse. The two trigger power supplies can be delayed relative to one another by means of a variable delay. Figure 2 shows typical cross correlation measurements obtained by varying the relative delays of the crystal gate and the MCP gate. From such measurements one can determine the relative delay necessary in order to achieve optimum synchronization between the two pulsed systems.

With zero voltage on the  $KD^*P$  crystal and an ideal, perfectly collimated light beam at normal incidence, no light should leak through the shutter with crossed polarizers. However, in practice beams with a finite divergence will not be uniformly retarded in the birefringent crystal resulting in light leakage and subsequent decrease in contrast ratio. For diagnostic purposes using photographic techniques, this could be a serious drawback if one integrates the light flux over too long a period of time  $\Delta\tau_2$ . The contrast  $C$  obtained for a gate of width  $\Delta\tau_1$  on the crystal can be defined as :  $C = (T_{on}\Delta\tau_1/T_{off}\Delta\tau_2) - 1$ , where  $T_{on}$  is the relative transmission of the electrooptic shutter with the voltage applied across the crystal, and  $T_{off}$  is the leakage transmission with zero applied voltage. One finds<sup>9</sup> that for an incident beam divergence of 1°,  $T_{on}/T_{off} \simeq 100$ . Thus, the pulse length  $\Delta\tau_2$  of the MCP must be shorter than 12.5 ns to achieve a contrast  $C > 5$  for a  $KD^*P$  gate  $\Delta\tau_1 = 750$  ps ; otherwise the film will be excessively fogged by the background leakage light. This illustrates the critical role played by the MCP. The optimization of the beam divergence is achieved by means of the collimating optics shown in Fig. 1 (Photographs 4a and 4c illustrate the overall photon leakage of the device for a 750 ps gate).

Our time-resolved diagnostic is ultimately dependent on the almost instantaneous Čerenkov radiation<sup>10</sup> generated by the electron beam incident on the Plexiglass sheet. Long lived emission mechanisms such as fluorescence must be weak or nonexistent. To check this we study the light generated when a  $\sim 100$  A, 100–250 kV electron beam of 500 ns duration impinges on the Plexiglass screen. The light intensity emitted on-axis is measured with a photomultiplier tube having a subnanosecond time resolution. As is seen

from the insert in Fig. 3, the structure of the light pulse follows closely the voltage pulse of the electron beam. No long lived slow component of the light pulse is observed.

We also see in the insert of Fig. 3 that whereas the voltage pulse decays slowly as a result of an RC droop in the Marx generator, the light intensity falls off abruptly when a certain voltage is reached. This effect is related to the well known Čerenkov threshold  $nv_{\parallel} \geq 1$ , where  $n$  is the refractive index of Plexiglass and  $v_{\parallel}$  is the axial electron velocity. As the accelerator voltage falls, so does  $v_{\parallel}$  until the threshold value  $nv_{\parallel} = 1$  is reached, at which point the emission suddenly stops.

A more accurate measurement of the threshold is obtained by varying the charging voltage of the Marx, thus changing the accelerating voltage of the beam. In figure 3, we plot the intensity of radiation measured by the PM tube as a function of the accelerating potential applied across the anode cathode gap ; the curve shows clearly a very steep onset around 110 kV, in very good agreement with the 120 kV predicted for the Čerenkov threshold. In addition to these photometric measurements, we have also made rough measurements of the wavelength of the light emitted on-axis by using a quartz prism as a dispersive element. The results indicate that most of the radiation is in the violet and UV part of the spectrum. From this measurement we find that the radiation wavelength lies in the interval 150-200 nm. The corresponding index of refraction  $n$  for Plexiglass lies in the range 1.70–1.62. The respective voltage thresholds are 120 and 139 kV.

Our time resolved emittance measurements are performed on a 2 MV, 1 kA, 30 ns electron beam generated in a multielectrode gun provided with a field emission cathode<sup>6</sup>. In the “pepper-pot” technique used<sup>6,7</sup>, the electron beam impinges on an array of 25 pinholes apertures in a 1 mm thick tantalum disk placed in the beam path. The apertures, each 0.5 mm in diameter are separated by a distance of 0.7 cm in a  $5 \times 5$  square pattern. The transmitted beamlets, each carrying a current of  $\sim 0.1$  A traverse a field free region 35 cm in length before they strike the blackened Plexiglass Čerenkov emitter. The remainder of the optics is as shown in Fig. 1.

Figure 4 shows successive pictures of the beamlets each obtained with a 750 ps time resolution. We see that the initial 1–3 ns turn-on period during which large beam spreading occurs, is followed by a relatively constant period in which the spot sizes are small and the emittance is thus low. A discussion of these and related studies will be given in separate

publication.

Finally we address the stability of a rotating, mildly relativistic electron ring (200 kV, 100 A, 500 ns) obtained by injecting an annular nonrotating electron beam into a magnetic cusp<sup>11</sup>. The beam is initially generated from a cylindrical knife-edge field emission cathode 6 cm in radius and of  $\sim 1$  mm thickness. Rotation is achieved by injection into a magnetic cusp with upstream and downstream magnetic fields equal to +250 G and -250 G, respectively.

Figure 5 shows a few selected pictures produced with a 2ns gate at different times in the pulse history. The photographs on the left correspond to the space charge evolution of the beam, in the absence of magnetic field (no rotation) ; those on the right are obtained for  $|B_z| \simeq 250$  G. In both cases the length of the drift region after the cusp is 10 cm. The first set of pictures, taken on the rise of the pulse ( $t \simeq t_0$ ), show the turn-on of the knife-edge field emission cathode : a few hot spots appear, while the ring is not formed yet.. At time  $t - t_0 \simeq 100$  ns, the electron ring is formed and shows a very regular structure. Later in the pulse, the images obtained with and without magnetic field are quite different : a double ring structure appears, only in the presence of  $B_z$ , and can be explained by the coherent off-centering process discussed by Destler *et al*<sup>12</sup>. Finally, at the end of the pulse ( $t - t_0 \simeq 500$  ns), the beam shows bunching, which is observed only in the presence of the magnetic field, and is probably related to the diocotron instability<sup>1</sup>. At  $t - t_0 \simeq 700$  ns, the voltage RC decays below 110 kV and the light emission stops, having reached the Čerenkov threshold.

In conclusion, we have presented a new diagnostic device coupling the Čerenkov emission process to the electrooptic effect and we demonstrated its capability in obtaining two dimensional images of electron beams with subnanosecond time resolution. The technique is applicable even for the case of mildly relativistic electron beams with energies as low as  $\sim 120$  kV. It surpasses the conventional streak camera which is a one dimensional device, since one axis is lost to the streak process.

Several considerations limit the ultimate time resolution of our diagnostic. First, the ability to generate very short high voltage pulses ( $\sim$  kV/ps) to energize the electrooptic crystal, secondly the time response of the crystal itself (buildup of the electrooptic effect), and finally our ability to achieve a sufficiently good contrast  $C$ . We believe that time

resolutions as short as  $\sim 50$  ps with a contrast  $C > 5$  can be achieved. However, a great deal depends on the amount of Čerenkov light that is available. To illustrate this point, consider the emittance experiment described above. The 2 MeV beam with a current density of  $100 \text{ A/cm}^2$  generates in our Čerenkov plate (effective thickness  $\simeq 3$  mm) a radiation flux of  $\sim 40 \text{ kW/cm}^2$  in the wavelength range 300–600 nm. However, each beamlet on the downstream side of the pepper-pot screen carries only 0.1 A and gives rise to only 40 W of light. After collimation, polarization and aperturing of the light beam, the average number of photons transmitted during a 750 ps gate to a microchannel is estimated as  $\sim 100$ . At this level the quantum efficiency of the MCP plays a significant role and the system works basically as a photon counter, thus introducing a certain grainyness in the pictures. On the other hand in our studies of the rotating electron ring, light intensity does not pose a problem. The 200 keV, 100 A electron beam generates  $\sim 25 \text{ kW}$  of light in the 300-600 nm wavelength range (effective plate thickness  $\sim 10$  mm).

This work was supported by the Lawrence Livermore National Laboratory, the Air Force Office of Scientific Research, the National Science Foundation and the Department of Energy. One of us (F. H.) also gratefully acknowledges useful technical assistance from Dr. H. Lamela Rivera.

## References

- [1] R.C. Davidson, *Theory of Nonneutral Plasmas* (Benjamin, Reading, MA., 1974)
- [2] C. Lejeune and J. Aubert, in *Applied Charged Particles Optics*, edited by A. Septier (Academic, New York, 1980)
- [3] C.W. Roberson, Proc. Soc. Photo-Opt. Int. Eng., **453**,320 (1983)
- [4] C. Lee, P.E. Ottinger, A. Sliski and M. Fishbein, Rev. Sci. Instr., **56**,560 (1985)
- [5] C. Lee and P.E. Ottinger, J. Appl. Physics, **58**,1996 (1985)
- [6] D.A. Kirkpatrick, R.E. Shefer and G. Bekefi, J. Appl. Physics, **57**,5011 (1985)
- [7] G. Bekefi, R.E. Shefer and S.C. Tasker, Proc. 7<sup>th</sup> International F.E.L. Conf., Tahoe City, CA. (1985)
- [8] F. Hartemann, G. Bekefi and W.W. Destler, Bull. APS, **30**,1635 (1985)
- [9] F. Zernike and J.E. Midwinter, *Applied Nonlinear Optics* (Academic Press, New York 1974)
- [10] V.P. Zrelov, *Cherenkov Radiation in High Energy Physics* (Israel Program for Scientific Translation, Jerusalem 1970)
- [11] M.J. Rhee and W.W. Destler, Phys. Fluids, **17**,1574 (1974)
- [12] W.W. Destler and M.J. Rhee, Phys. Fluids, **20**,1582 (1977)

## Figure captions

**Fig. 1** Overall experimental setup.

**Fig. 2** Light intensity as a function of the relative delay between the optical gate and the 12 ns wide MCP gate. The solid circles are for a 4 ns optical gate, the open circles for a 1 ns gate.

**Fig. 3** Radiation intensity on-axis as a function of the diode voltage. Insert : Time-history of the voltage and light intensity emitted on-axis (The flat top voltage is 150 kV and the voltage pulse length is 1  $\mu$ s). The arrows indicate the Čerenkov threshold.

**Fig.4** Beamlet images in the emittance measurements ; (a) Light leakage 10 ns into the electron beam pulse with electrooptic modulator closed (b) same with 750 ps gate open at 1ns ; (c) at 10 ns ; (d) at 20 ns.

**Fig.5** Photographs of the ring electron beam obtained at different times (a) 0 ns, (b) 100 ns, (c) 500 ns into the pulse with a 2 ns gate, with and without the cusp magnetic field.

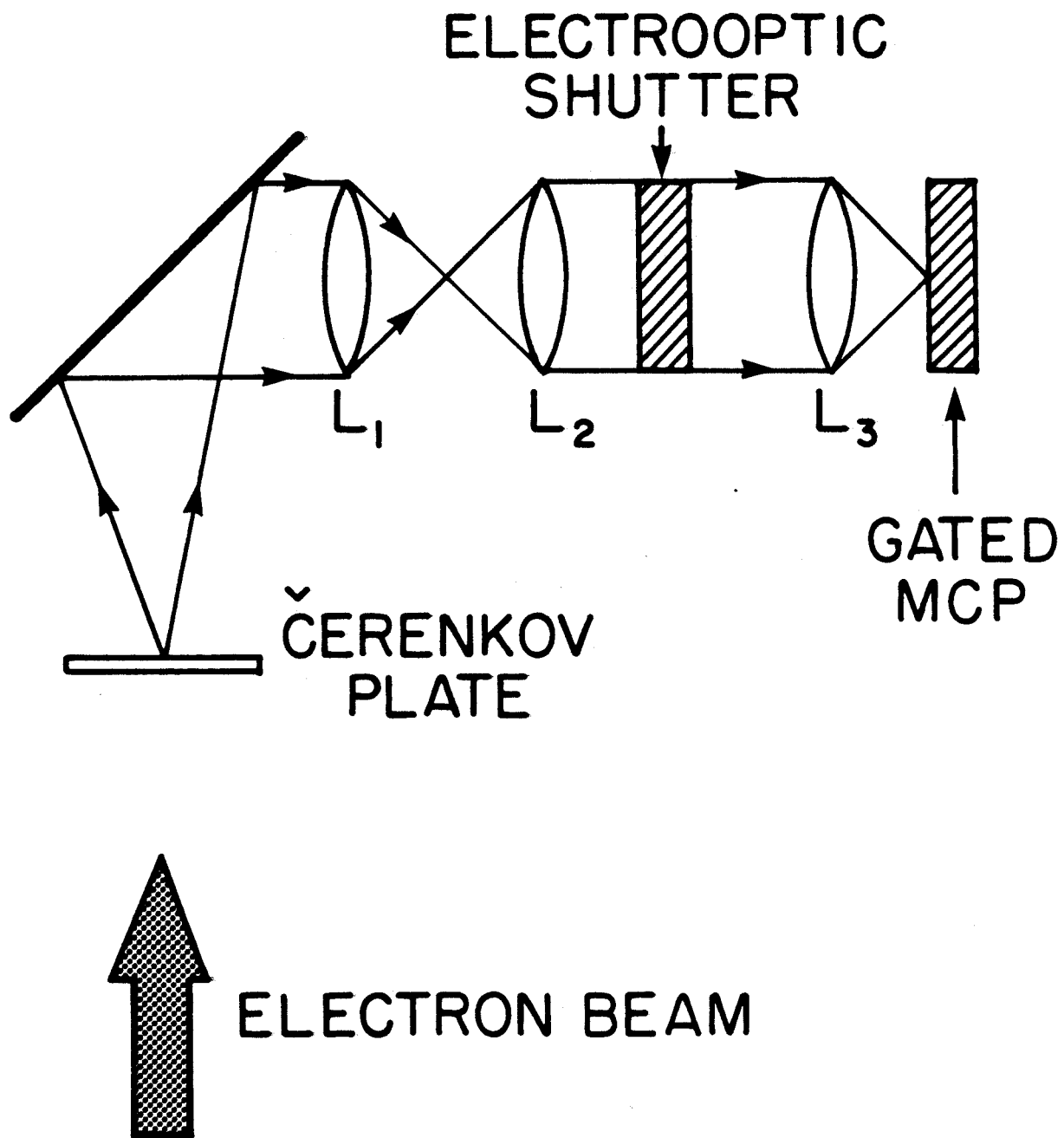


Fig. 1  
Hartemann & Bekefi

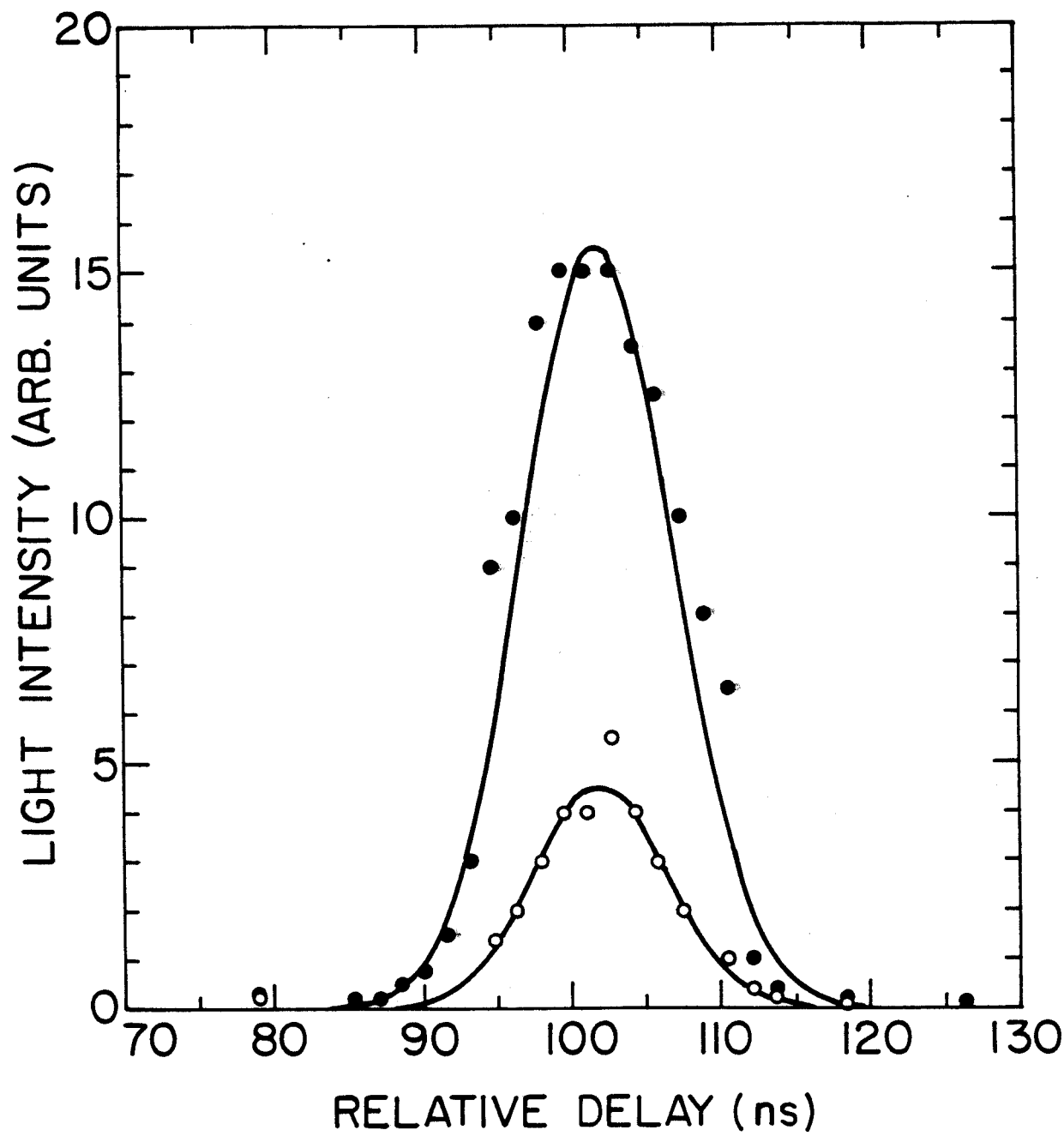


Fig. 2  
Hartemann & Bekefi

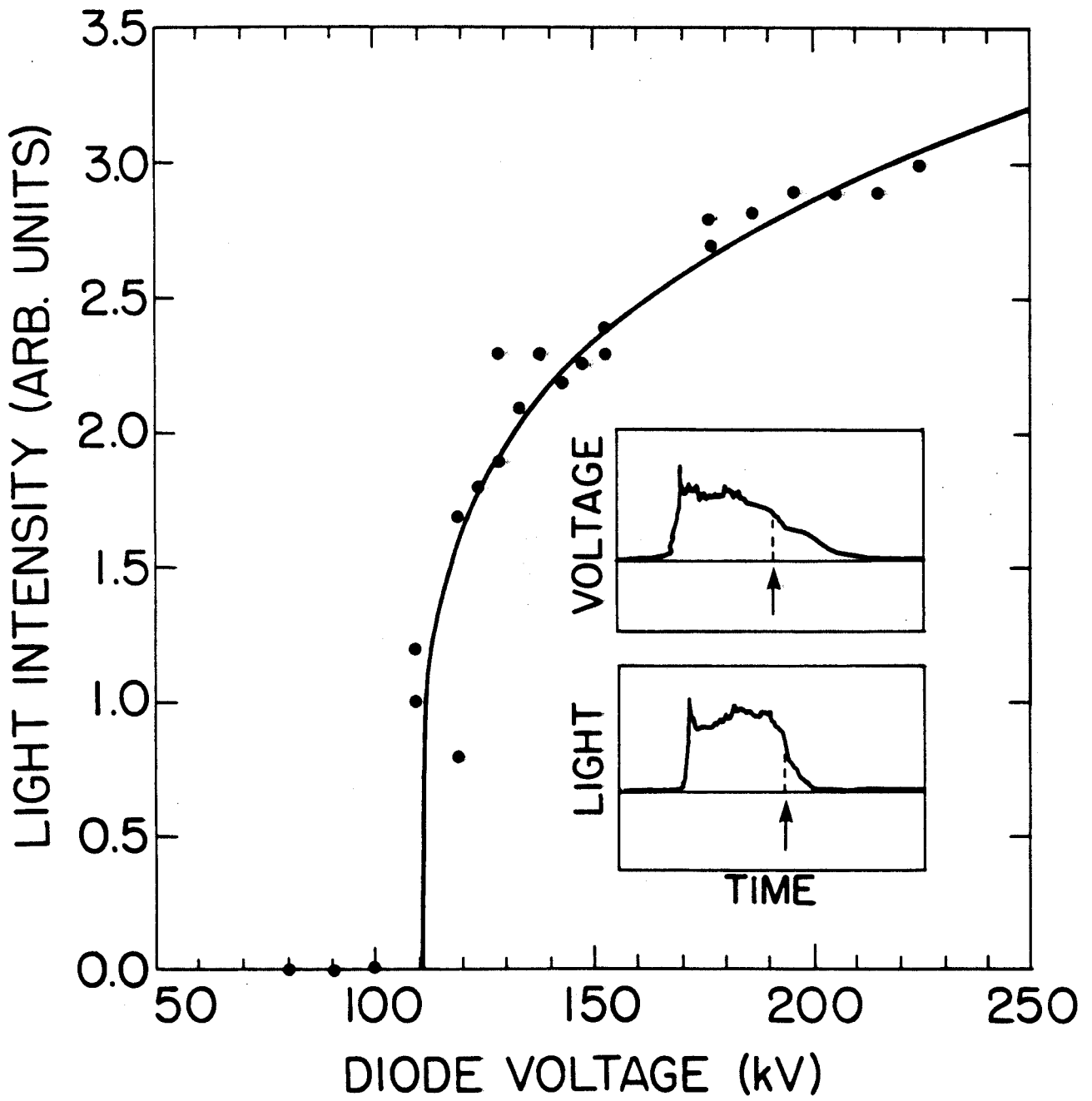
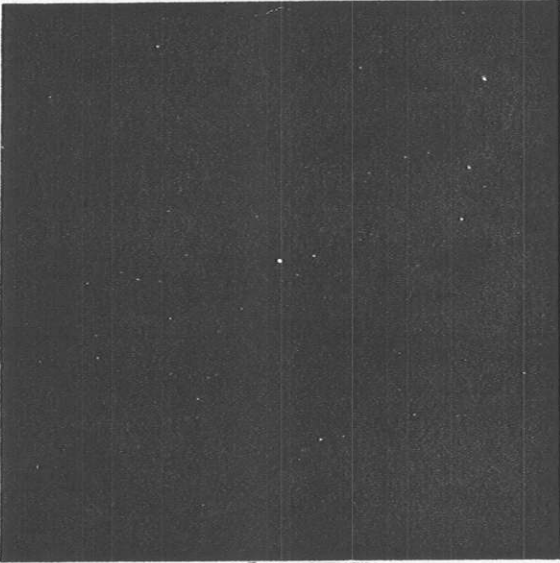


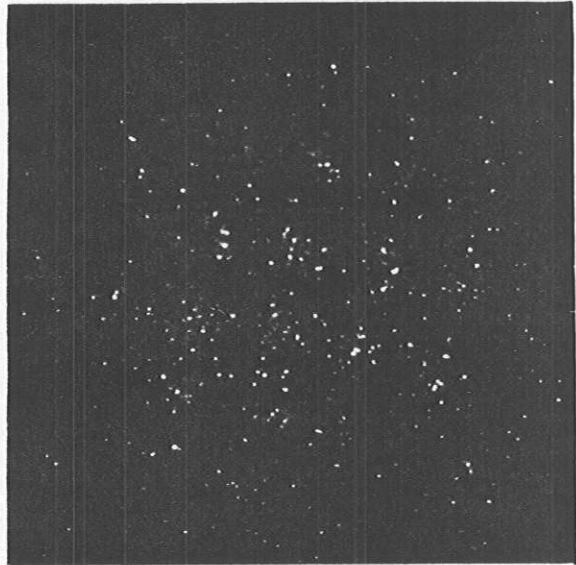
Fig. 3  
Hartemann & Bekefi

SS 19078

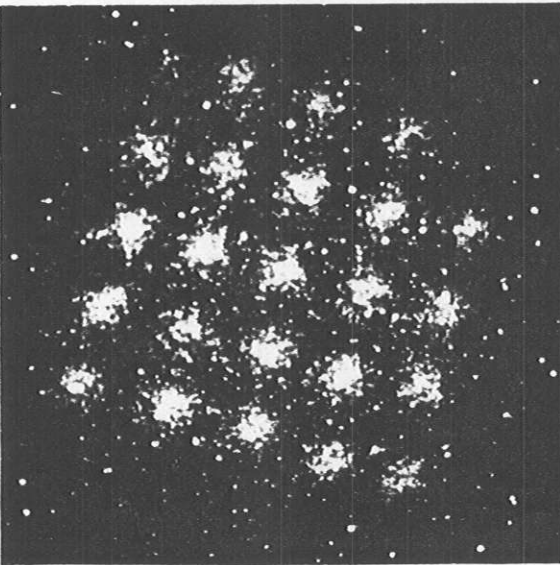
a



b



c



d

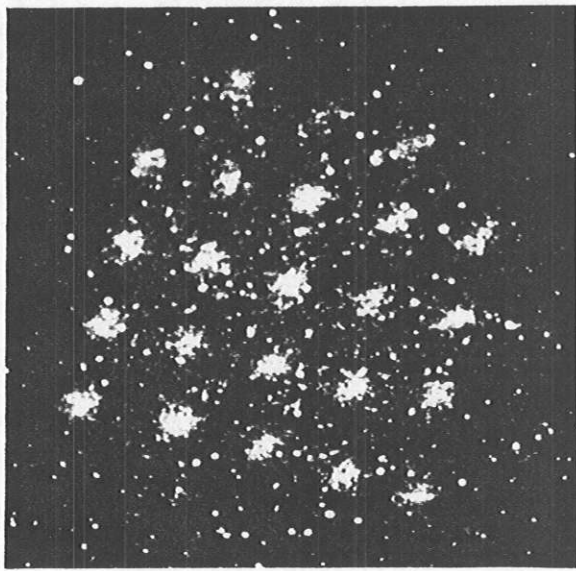
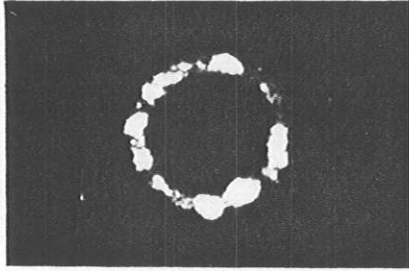


Fig. 4  
Hartemann & Bekefi

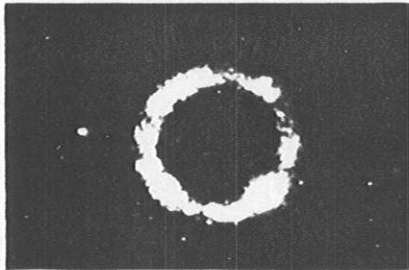
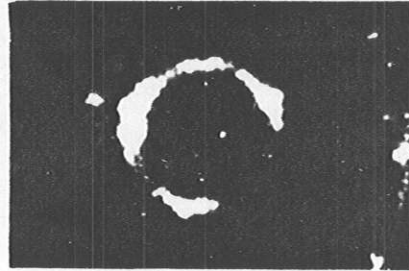
SS!  
1 HT. 19078

$B_z=0$

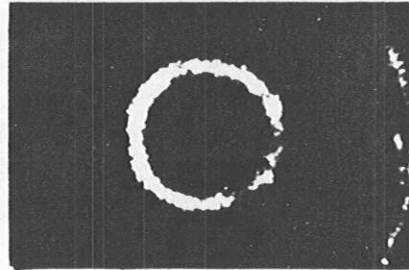
$B_z=250G$



a



b



c

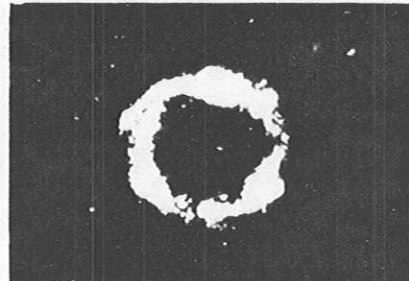


Fig. 5  
Hartemann & Bekefi

SS-19078